Cancer Cell
Article

Oncogenic BRAF Induces Melanoma Cell Invasion by Downregulating the cGMP-Specific Phosphodiesterase PDE5A

Imanol Arozarena,[1,3] Berta Sanchez-Laorden,[1] Leisl Packer,[1] Cristina Hidalgo-Carcedo,[2] Robert Hayward,[1] Amaya Viros,[1] Erik Sahai,[2] and Richard Marais[1,*]
[1]The Institute of Cancer Research, Signal Transduction Team, Section of Cell and Molecular Biology, 237 Fulham Road, London SW3 6JB, UK
[2]Tumour Cell Biology Laboratory, CR-UK LRI, 44 Lincoln's Inn Fields, London WC2A 3PX, UK
[3]Present address: Faculty of Life Sciences, Michael Smith Building, University of Manchester, Manchester M13 9PT, UK
*Correspondence: richard.marais@icr.ac.uk
DOI 10.1016/j.ccr.2010.10.029

SUMMARY

We show that in melanoma cells oncogenic BRAF, acting through MEK and the transcription factor BRN2, downregulates the cGMP-specific phosphodiesterase PDE5A. Although PDE5A downregulation causes a small decrease in proliferation, its major impact is to stimulate a dramatic increase in melanoma cell invasion. This is because PDE5A downregulation leads to an increase in cGMP, which induces an increase in cytosolic Ca^{2+}, stimulating increased contractility and inducing invasion. PDE5A downregulation also this leads to an increase in short-term and long-term colonization of the lungs by melanoma cells. We do not observe this pathway in NRAS mutant melanoma or BRAF mutant colorectal cells. Thus, we show that in melanoma cells oncogenic BRAF induces invasion through downregulation of PDE5A.

INTRODUCTION

Melanocytes are specialized pigment cells located primarily in the skin, where they determine complexion and hair color and provide protection from the damaging effects of ultraviolet radiation (Gray-Schopfer et al., 2007; Kasper et al., 2007). These cells are also the precursors of melanoma, a potentially deadly skin cancer that kills about 8,000 people in the United States and about 12,000 people in Europe each year. In many Western societies, melanoma incidence almost doubles every decade. If treated early, melanoma can be cured by surgical resection, but due to its proclivity to metastasize, in about 20% of patients it progresses to an aggressive invasive disease that is refractory to treatment and has a poor prognosis, with median survival rates of 6–9 months and 5 year survival rates of 5%–10%. These data highlight the need for improved understanding of melanoma biology to facilitate development of therapeutic strategies.

An important signaling pathway in melanoma is the RAS/RAF/MEK/ERK cascade (Gray-Schopfer et al., 2007). RAS is a small G protein that is activated downstream of growth factor, cytokine, and hormone receptors. RAF is a serine/threonine-specific protein kinase that is activated downstream of RAS. RAF phosphorylates and activates another protein kinase called mitogen and extracellular signal-regulated protein kinase kinase (MEK), which in turn activates a third protein kinase called extracellular signal-regulated protein kinase (ERK). In normal cells, this pathway regulates proliferation, senescence, survival, and differentiation, whereas in cancer it is constitutively activated, and survival and proliferation are the favored outcomes.

There are three *RAS* (*HRAS*, *KRAS*, *NRAS*) and three *RAF* (*ARAF*, *BRAF*, *CRAF*) genes in humans (Gray-Schopfer et al., 2007). About 25% of melanomas carry oncogenic mutations in *RAS* (primarily *NRAS*), and a further 44% carry oncogenic mutations in *BRAF* (http://www.sanger.ac.uk/genetics/CGP/cosmic/). The most common BRAF mutations in melanoma (90% of cases with BRAF mutations) involve a glutamic acid substitution for valine 600 (V600E) (Davies et al., 2002), and abundant data validate ^{V600E}BRAF as a therapeutic target in

Significance

The protein kinase BRAF is activated by somatic gain-of-function mutations in about 44% of human melanomas. This results in ERK pathway hyper-activation, and we show that this leads to downregulation of PDE5A, a cGMP-selective phosphodiesterase. PDE5A is the target of drugs such as sildenafil, tadalafil, and vardenafil, which are used to treat erectile dysfunction and pulmonary arterial hypertension. PDE5A downregulation by ^{V600E}BRAF induces melanoma cell invasion in vitro and in vivo and increased long-term colonization of the lungs by melanoma cells. PDE5A inhibition by sildenafil induces invasion in vitro but does not increase lung colonization. Our study establishes a link between PDE5A, cGMP, and Ca^{2+} metabolism, and the regulation of invasion by oncogenic BRAF in melanoma cells.

melanoma (Hingorani et al., 2003; Karasarides et al., 2004; Liang et al., 2007). BRAF-selective drugs can achieve dramatic clinical responses in patients who have melanomas that express mutant BRAF, although most patients appear to eventually relapse on treatment (Flaherty et al., 2010). These data demonstrate the promise of BRAF drugs but also highlight the need to fully understand this pathway to overcome resistance and to learn how to use these drugs in effective combination therapies.

We recently performed expression array analysis in melanoma cells and demonstrated that oncogenic BRAF upregulates expression of many genes but downregulates expression of a much smaller number (Packer et al., 2009). One of the genes identified as potentially downregulated by oncogenic BRAF in melanoma cells was the cyclic GMP (cGMP)-specific phosphodiesterase *PDE5A*. Cyclic AMP (cAMP) and cGMP are generated downstream of peptide hormone, cytokine, and other cell surface receptors. The intensity and duration of signaling by these second messengers is controlled by their relative rates of synthesis by adenylyl (cAMP) and guanylyl (cGMP) cyclases and their rates of degradation by a large family of phosphodiesterases (Omori and Kotera, 2007).

Classically, cGMP is implicated in phototransduction in retinal cells and in relaxation of the smooth muscle cells lining the veins. However, in other cells cGMP modulates glyconeogenesis, ion channel conductance, proliferation, and apoptosis. It regulates two protein kinases (PRKG1 and PRKG2), several Ca^{2+} channels, and the cAMP-specific phosphodiesterases PDE2, PDE3A, and PDE3B (Biel and Michalakis, 2009; Mongillo et al., 2006; Pilz and Broderick, 2005). Through alternative splicing, the *PDE5A* gene produces three proteins (PDE5A1, PDE5A2, and PDE5A3) that differ in their N termini and range in mass from 95 to 105 kDa (Lugnier, 2006). PDE5A1 and PDE5A2 are ubiquitous, whereas PDE5A3 is restricted to vascular smooth muscle (VSM) cells (Lin et al., 2006). Importantly, PDE5A is the therapeutic target of drugs including sildenafil (Viagra), vardenafil (Levitra), and tadalafil (Cialis) that are used to treat erectile dysfunction and pulmonary arterial hypertension (Ghofrani et al., 2006).

Previous studies have established that there is crosstalk between RAS/RAF and cAMP signaling in melanoma cells (Dumaz and Marais, 2005), but the role of cGMP in melanoma is poorly characterized. The identification of PDE5A as a possible transcriptional target of ^{V600E}BRAF suggests that cGMP metabolism is regulated by oncogenic BRAF, and the aim of this study was to investigate the role of this second messenger in melanoma cells.

RESULTS

Oncogenic BRAF Downregulates PDE5A in Melanoma Cells

To investigate the role of cGMP in melanoma, we first wished to confirm that PDE5A is downregulated by oncogenic BRAF in melanoma cells. Using qRT-PCR, we show that BRAF depletion with two small-interfering RNA (siRNA) probes or BRAF inhibition with the selective inhibitors PLX4720 or SB590885 caused a substantial (5- to 8-fold) increase in PDE5A mRNA in ^{V600E}BRAF-expressing A375P melanoma cells (Figure 1A). MEK inhibition by U0126 or PD184352 also caused a 6- to 12-fold increase in PDE5A mRNA (Figure 1A). Similar results were seen in ^{V600D}BRAF-expressing WM266.4 cells (Figure 1B), confirming that oncogenic BRAF downregulates PDE5A in melanoma cells.

In agreement with PDE5A downregulation by oncogenic BRAF, relative to diploid normal human melanocytes (NHMs), PDE5A mRNA is strongly downregulated in nine out of ten melanoma lines expressing oncogenic BRAF, with only 501mel cells expressing similar levels to NHM (Figure 1C). We also show that PDE5A protein is downregulated in eight of these lines, and by Western blot is only detectable in 501mel and, albeit weakly, Skmel24 cells (Figure 1D). However, note that PD184352 and U0126 still increase PDE5A mRNA and protein in 501mel and Skmel24 cells (Figure 1E), demonstrating that even in these cells ^{V600E}BRAF/MEK downregulates PDE5A.

Oncogenic BRAF Downregulates PDE5A1 through BRN2

Next, we investigated how ^{V600E}BRAF regulates PDE5A expression in melanoma cells. We previously reported that ^{V600E}BRAF upregulates expression of the POU-domain transcription factor BRN2 (POU3f) in melanoma cells (Goodall et al., 2004). In silico analysis (http://www.cbrc.jp/research/db/TFSEARCH.html) of the *PDE5A* promoter revealed two putative BRN2-binding sites at −890/−870 and −720/−690 relative to the transcription start site (Figure 2A). Using chromatin immunoprecipitation (ChIP) assays, we show that BRN2 was bound to the PDE5A promoter in both A375P (Figure 2B) and Skmel13 (Figure 2C) cells. To demonstrate the specificity of the antibody used for these studies, we show that the *PDE5A* promoter was not immunoprecipitated by this antibody when BRN2 was depleted using siRNA (Figure 2C) and that BRN2 did not bind to a region of the promoter away from the putative BRN2-binding sites (see Figure S1 available online).

To examine directly PDE5A transcriptional regulation by BRAF, we cloned a 1080 bp fragment upstream of the transcription start site of the *PDE5A* promoter into the promoter-less luciferase reporter vector pGL2 (−1080wt) (Figure 2A). We also generated a version of this reporter in which the putative BRN2 site at −720 was mutated (−1080mut) (Figure 2A) and a version consisting of a 497 bp upstream fragment that lacks both sites (−497) (Figure 2A). In A375 cells the promoters lacking the putative −720 site (−1080mut, −497) both had higher basal activity than the wild-type (−1080wt) promoter (Figure 2A). Moreover, whereas the activity of the −1080wt promoter increased significantly following BRAF depletion using siRNA, or following BRAF or MEK inhibition with PLX4720 and PD184352, respectively, the −1080mut and −497 promoters were not significantly affected by BRAF depletion, or BRAF or MEK inhibition (Figure 2D). Furthermore, BRN2 depletion upregulated PDE5A mRNA and protein in several melanoma lines (Figures 2E and 2F), whereas its expression downregulated PDE5A in normal human melanocytes (Figure 2G). We conclude that BRN2, a transcription factor that is upregulated by oncogenic BRAF, directly suppresses PDE5A expression in melanoma cells.

PDE5A Regulates Melanoma Cell Invasion

We next tested if PDE5A regulates melanoma cell growth. Re-expression of PDE5A1 did not significantly affect A375 cell growth in vitro (Figure 3A), but it caused a small increase in WM266.4 cell growth (Figure 3B). Conversely, stable depletion

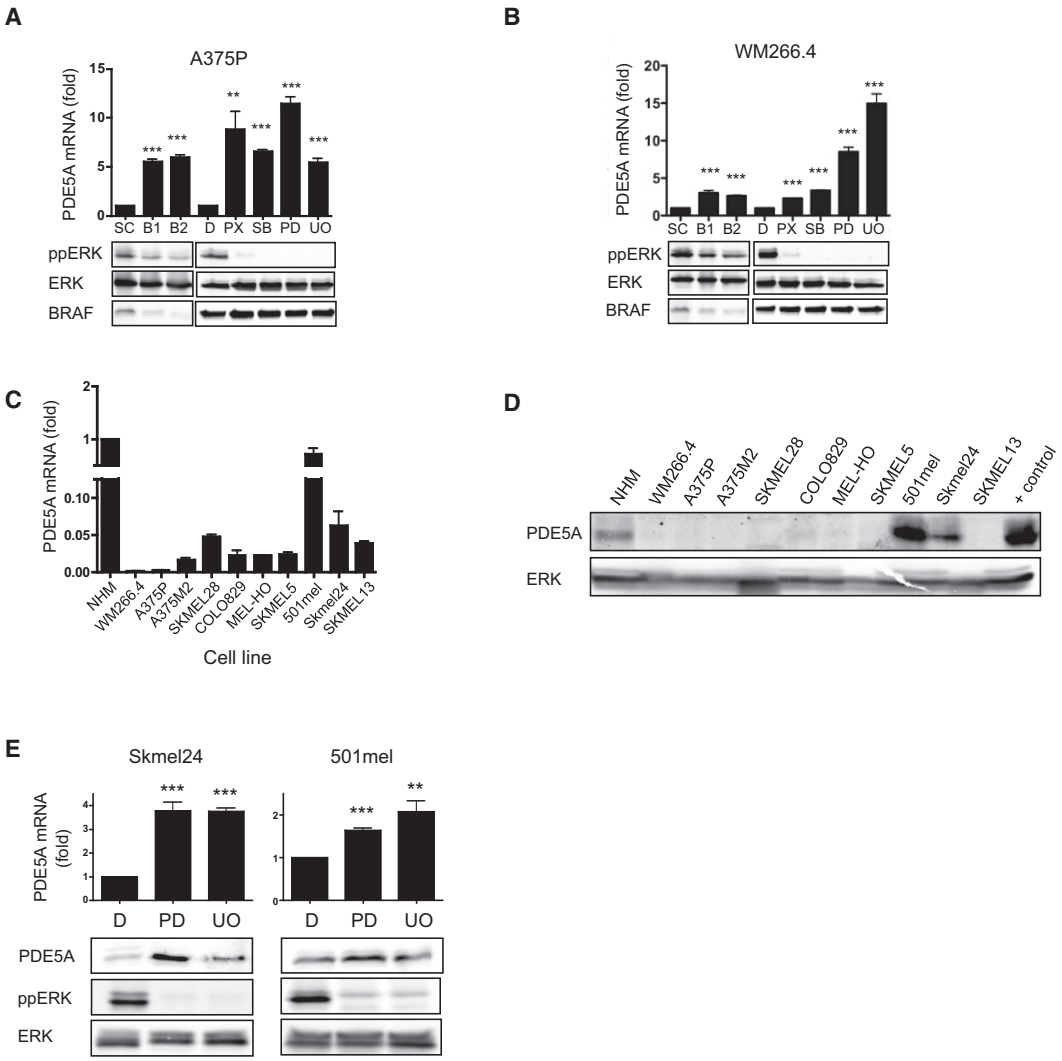

Figure 1. Oncogenic BRAF Downregulates PDE5A in Melanoma Cells

(A and B) A375P (A) and WM266.4 (B) cells were transfected with scrambled control (SC) or BRAF (B1, B2) siRNA for 48 hr, or treated with DMSO (D) PLX4720 (PX; 0.3 μM), SB590885 (SB; 0.3 μM), PD184352 (PD; 1 μM), or UO126 (UO; 10 μM) for 24 hr. PDE5A mRNA was measured by qRT-PCR. The results are relative to the scrambled control for siRNA or relative to DMSO for the drugs. The Western blots show phosphorylated ERK (ppERK), total ERK, and BRAF in the cell extracts. (C) PDE5A mRNA levels were measured by qRT-PCR in ten BRAF mutant melanoma lines. The levels are presented relative to those in normal diploid human melanocytes (NHM). (D) Western blot showing PDE5A protein in NHM and ten BRAF mutant melanoma lines with ERK2 (ERK) as a loading control. (E) Skmel24 and 501mel cells were treated with DMSO (D) PD184352 (PD; 1 μM) or UO126 (UO; 10 μM). PDE5A mRNA levels were determined by qRT-PCR and are presented relative to DMSO. The Western blots show PDE5A, phosphorylated ERK (ppERK), and ERK2 (loading control). Data are means of triplicate samples; error bars indicate ± standard error. ***$p < 0.001$, **$p < 0.01$.

of PDE5A using short-hairpin RNA (shRNA) caused a small decrease in growth of 501mel cells (Figure 3C). We observed similar effects in vivo: PDE5A re-expression did not affect growth of A375 xenografts in nude mice (Figure 3D) but increased growth of WM266.4 xenografts (Figure 3E). Note that the lack of effect in A375 cells was not because PDE5A expression was lost during in vivo culture (Figures 3F and 3G), and we were unable to examine how PDE5A depletion affected 501mel cell growth in vivo because they do not grow as xenografts.

Thus, although PDE5A provides a small growth advantage to some melanoma cells, it is nevertheless downregulated in the majority of the cell lines we examined, suggesting that it regulates functions other than growth. Recent studies have shown that ^{V600E}BRAF and BRN2 both regulate melanoma cell invasion (Goodall et al., 2008; Pinner et al., 2009), and because we show here that they also both regulate PDE5A expression, we investigated if PDE5A regulates melanoma cell invasion. Using a recently described approach (Sanz-Moreno et al., 2008), we confirm that PLX4720, SB590885, PD184352, and U0126 all strongly suppressed WM266.4 cell invasion into collagen I matrices in vitro (Figure 4A). Furthermore, we show that BRAF and BRN2 depletion also inhibited invasion of these cells (Figure 4B). Importantly, stable (Figure 4C) or transient (Figure S2A) re-expression of PDE5A1, PDE5A2, or PDE5A3 strongly

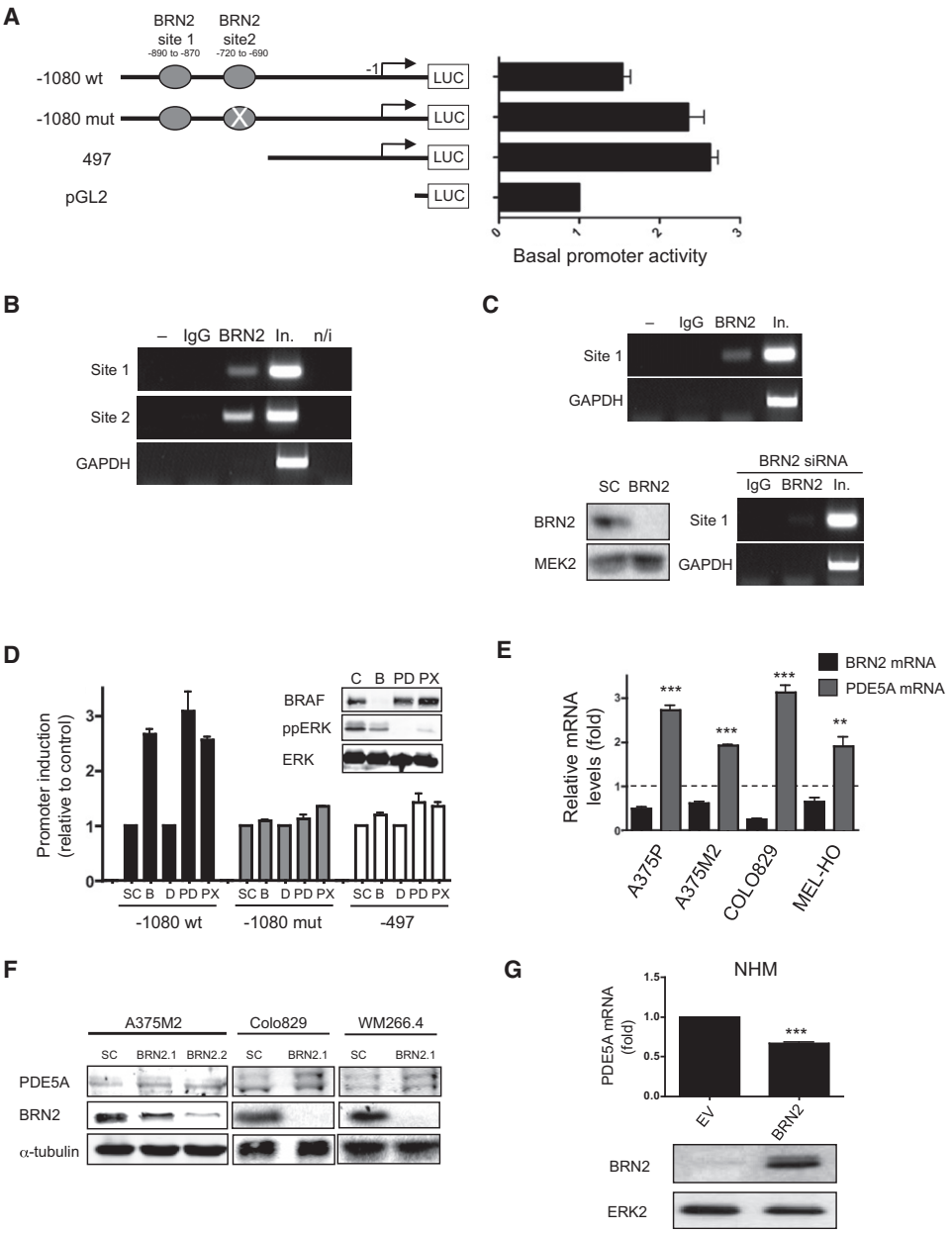

Figure 2. BRN2 Downregulates PDE5A

(A) Schematic representing *PDE5A1* promoter reporter constructs. The promoter fragments span the 1080 (−1080wt) or 497 (−497) bp region upstream of the transcription start site. The position of two putative BRN2-binding sites is indicated, and in the −1080mut construct, the putative site at −720 is mutated (X). Promoter-less pGL2 is also represented. To the right the basal activity of these reporter constructs is shown relative to pGL2. Data are the average for one experiment measured in triplicate with error bars to show standard deviations from the mean. (B) ChIP assays from A375P cells using no antibody (–), nonspecific antibody (IgG), or BRN2 antibody (BRN2). Controls of direct amplification of input DNA (In.) and no input DNA (n/i) are shown. The regions spanning −890 to −870 (Site 1) and −720 to −690 (Site 2) of the PDE5A promoter were amplified, with the GAPDH promoter as the internal control. (C) ChIP assays from SkMel13 cells using no antibody (–), nonspecific antibody (IgG), or BRN2 antibody (BRN2). Direct amplification of input DNA (In.) was included as a control. The region spanning −890 to −870 (Site 1) of the PDE5A promoter was amplified, with the GAPDH promoter as an internal control. The upper panel shows specific capture of this promoter region. In the lower panels, Skmel13 cells were transfected with scrambled (SC) or BRN2 (BRN2) siRNA. The left panel shows a Western blot for BRN2 and MEK2 (loading control) to confirm efficient BRN2 knockdown, and the right panel shows the ChIP assay using nonspecific (IgG) or the BRN2 antibody (BRN2). (D) PDE5A (−1080wt, −1080mut, and −497) promoter activity was measured by luciferase assay in A375 cells transfected with scrambled control (SC) or BRAF (B) siRNA, or treated with DMSO (D), PLX4720 (PX: 0.3 μM), or PD184352 (PD: 1 μM). Extracts were prepared 48 hr after siRNA transfection, or 24 hr after addition of PLX4720 or PD184352. The BRAF siRNA transfected sample activity is relative to the scrambled control, whereas PLX4720 and PD184352 activity is relative to DMSO-treated cells. Data are the average of triplicate measurements for one experiment with error bars to represent standard deviations from the mean. The inset shows a Western blot for BRAF, phospho-ERK2, and ERK2 (loading control) in the cell lysates. (E) Melanoma cell lines were transfected with BRN2 siRNA for 48 hr, and the relative levels of BRN2 (black) and PDE5A (gray) mRNA were measured by qRT-PCR. The results are presented relative to scrambled siRNA controls, which is represented by the dotted line. (F) A375M2, Colo829, and WM266.4 cells were transfected with scrambled control (SC) or BRN2

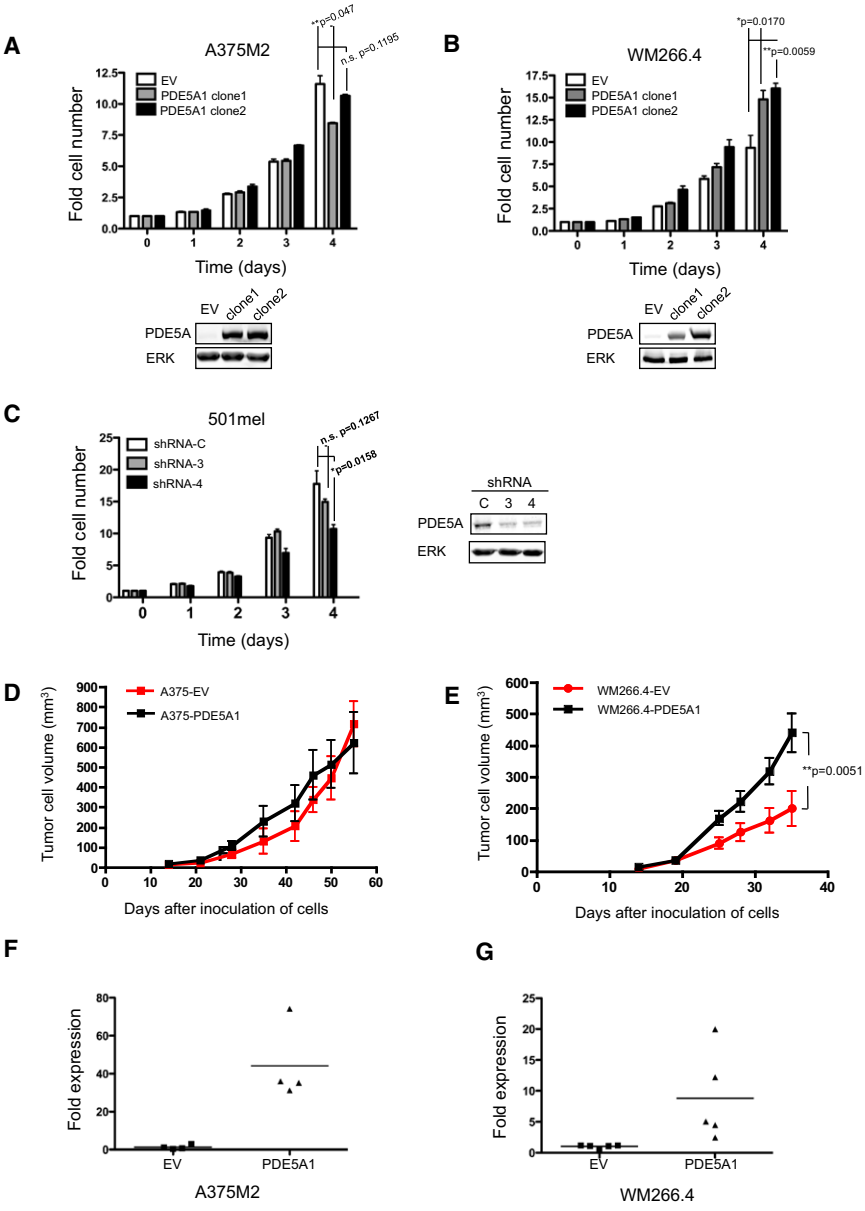

Figure 3. Effects of PDE5A on Melanoma Cell Growth

(A and B) The growth of A375M2 (A) or WM266.4 (B) cell clones engineered for stable re-expression of PDE5A1 or an empty vector control (EV) was measured over 4 days. Data are the means of triplicate samples with error bars to represent standard error. The Western blots show expression of PDE5A and ERK2 (loading control). (C) The growth of 501mel cell clones engineered for stable expression of PDE5A-targeting shRNA (shRNA-3, shRNA-4) or a control shRNA (shRNA-C) was measured over 4 days. Data are the means of triplicate measurements with error bars to represent standard error. The Western blots show expression of PDE5A1 and ERK2 (loading control). (D) The growth of tumor xenografts formed from A375M2 cells expressing PDE5A1 (A375-PDE5A1) or empty vector (A375-EV) in nude mice is shown. The results show mean volumes for groups of five animals with error bars to represent standard error. (E) The growth of tumor xenografts formed from WM266.4 cells expressing PDE5A1 (WM266.4-PDE5A1) or empty vector (WM266.4-EV) in nude mice is shown. The results show mean volumes for groups of five animals with error bars to represent standard error. (F) PDE5A mRNA levels for the tumor from (D) above were determined by qRT-PCR. (G) PDE5A mRNA levels for the tumor from (E) above were determined by qRT-PCR. Each data point represents the mean for an individual tumor analyzed in triplicate, and the bars represent the mean value for each group.

suppressed A375 and WM266.4 cell invasion. Conversely, we show that PDE5A depletion by siRNA enhanced 501mel and Skmel24 cell invasion (Figure 4D) and that the PDE5A inhibitors sildenafil, tadalafil, and vardenafil also increased 501mel cell invasion (Figure 4E). As important specificity controls for these experiments, we show that sildenafil, tadalafil, and vardenafil did not increase 501mel cell invasion when PDE5A was depleted by siRNA (Figure 4E) and that PDE5A siRNA, tadalafil, and sildenafil did not increase A375 or WM266.4 cell invasion (Figures 4F and 4G), consistent with the fact that these cells do not express PDE5A (Figures 1C and 1D). Thus, we conclude that PDE5A blocks invasion in BRAF mutant melanoma cells, and, therefore, when it is downregulated or inhibited, the cells invade.

To determine if ERK signaling regulates this pathway in other cells, we examined PDE5A expression and its regulation of invasion in RAS mutant melanoma cells (Figure S2B). Compared to NHM, PDE5A mRNA was substantially downregulated in three RAS mutant lines (WM1366, Skmel2, WM3629), was not downregulated in two others (WM852, Sbcl2), and was substantially upregulated in a sixth (WM1361). MEK inhibition increased PDE5A mRNA in WM1361 cells (Figure S2C), but PDE5A depletion in WM1361, Sbcl2, or WM3629 cells did not increase invasion substantially, and PDE5A re-expression in Skmel2 cells did not suppress invasion (Figure S2D). Thus, although oncogenic RAS downregulates PDE5A in melanoma cells, PDE5A does not appear to regulate invasion in this background. We also analyzed invasion and PDE5A expression in three BRAF mutant colorectal lines (HT29, Colo205, SW1417). BRAF and MEK inhibitors

(BRN2.1 and BRN2.2) siRNAs, and after 48 hr, lysates were Western blotted for PDE5A, BRN2, and α-tubulin (loading control). (G) NHMs were transiently transfected with an empty vector (EV) or a BRN2 expression construct for 48 hr. The relative levels of PDE5A mRNA were determined by qRT-PCR. The lower panels show Western blots for BRN2 and ERK2 (loading controls) in the cell lysates. Error bars indicate ± standard error. ***p < 0.001, **p < 0.01. See also Figure S1.

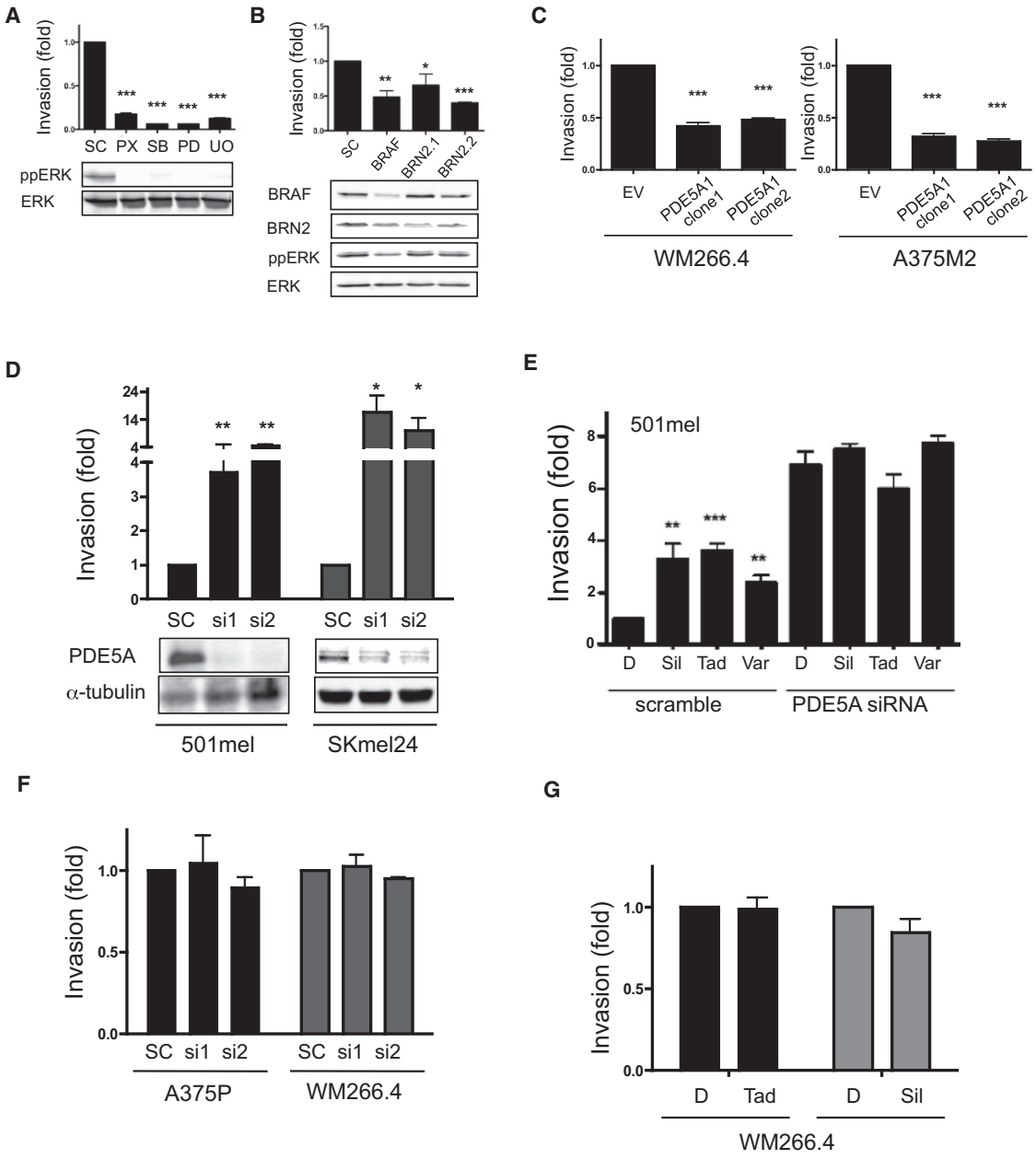

Figure 4. PDE5A1 Suppresses Melanoma Cell Invasion

(A) Invasion of WM266.4 cells in the presence of DMSO (D), PLX4720 (PX; 0.3 μM), SB590885 (SB; 0.3 μM), PD184352 (PD; 1 μM), or UO126 (UO; 10 μM). Invasion is presented relative to DMSO-treated control cells. The Western blots show phosphorylated (ppERK) and total ERK (loading control) in similarly treated cells. (B) Invasion of WM266.4 cells following transfection with scrambled control (SC), BRAF, or BRN2 (BRN2.1, BRN2.2) siRNA. The Western blots show BRAF, BRN2, phosphorylated ERK (ppERK), and ERK2 (loading control) in similarly treated cells. (C) Invasion of clones of A375M2 or WM266.4 cells engineered for stable expression of PDE5A1 or an empty vector control (EV). (D) Invasion of 501mel and Skmel24 cells following transfection with PDE5A (si1, si2) or scramble control (SC) siRNA. The Western blot shows PDE5A and α-tubulin (loading control) expression in transfected cells. (E) Invasion of 501mel cells following transfection with scrambled control (scramble) or PDE5A siRNA and treated with DMSO (D), sildenafil (Sil; 1 μM), tadalafil (Tad; 0.1 μM), or vardenafil (Var; 5 μM). (F) Invasion of A375P and WM266.4 cells following transfection with siRNA against PDE5A (si1, si2) or scrambled control (SC). (G) Invasion of WM266.4 cells treated with DMSO (D), tadalafil (Tad; 0.1 μM), or sildenafil (Sil; 1 μM). Error bars indicate ± standard error. ***p < 0.001, **p < 0.01, *p < 0.05. See also Figure S2.

downregulated PDE5A mRNA in HT29 cells and caused a small but insignificant upregulation in SW1417 cells and a significant upregulation in Colo205 cells (Figure S2E). Surprisingly, despite upregulating PDE5A in Colo205 and SW1417 cells, BRAF and MEK inhibitors increased rather than reduced invasion (Figure S2F). Note that HT29 cells do not invade and so could not be assessed (data not shown). Thus, although ^{V600E}BRAF does appear to downregulate PDE5A in some colorectal cells, it does not regulate invasion in these cells in the same manner as it does in melanoma cells.

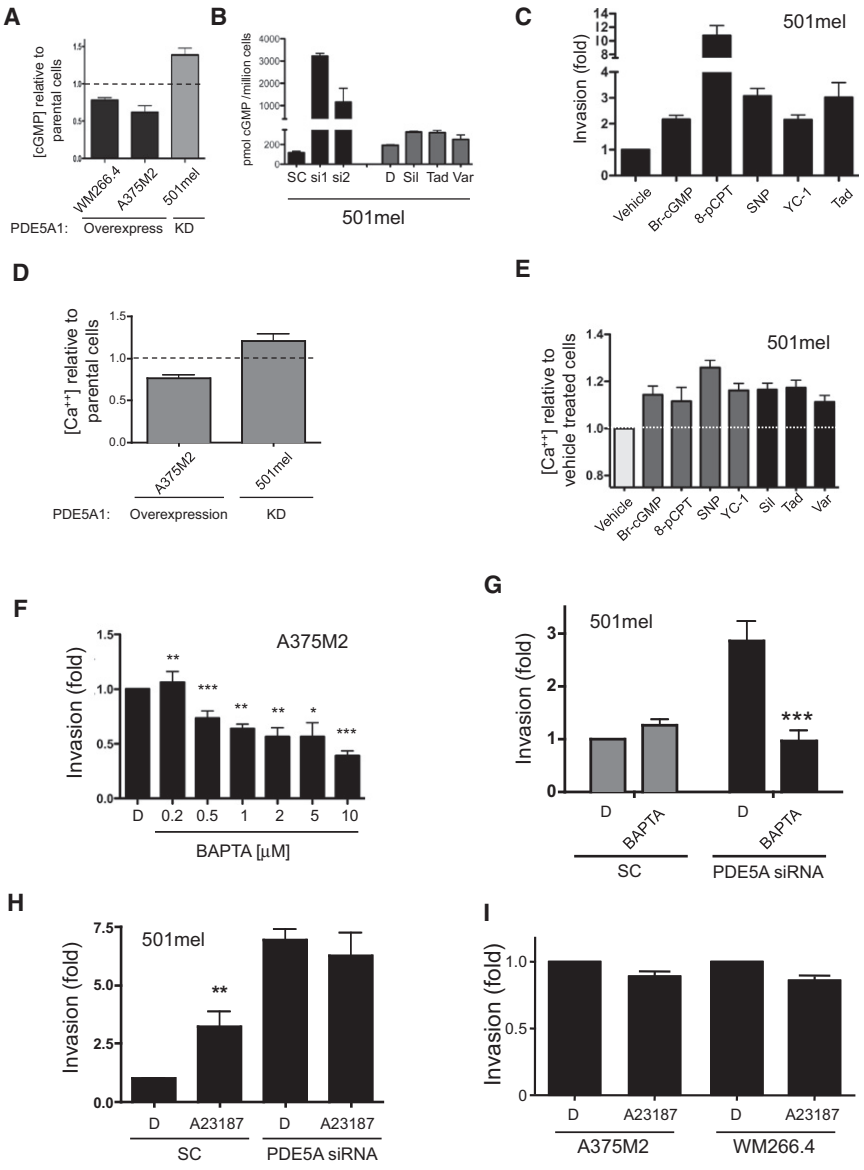

Figure 5. PDE5A Regulates Invasion through Ca^{2+} in Melanoma Cells

(A) Intracellular cGMP in WM266.4 or A375 clones re-expressing PDE5A1, or in a 501mel clone expressing PDE5A shRNA. The results are presented relative to their respective empty vector control clones (dotted line). (B) Intracellular cGMP in 501mel cells transfected with scrambled (SC) or two PDE5A siRNA (si1 and si2), or treated for 90 min with DMSO (D), tadalafil (Tad; 0.1 μM), sildenafil (Sil; 1 μM), or vardenafil (Var; 5 μM). cGMP levels are expressed as pMol cGMP/million cells. (C) Invasion of 501mel cells treated with Sp-8-Br-PET-cGMPS (Br-cGMP; 100 μM), 8-pCPT-cGMP (8-pCPT; 50 μM), sodium nitroprusside (SNP; 100 μM), or YC-1 (0.2 μM). The results are presented relative to vehicle-treated controls (H_2O for SNP; DMSO for all other compounds). As an experimental control, tadalafil (Tad; 0.1μM) treated cells are included. (D) Intracellular-free Ca^{2+} in an A375M2 clone re-expressing PDE5A1, and a 501mel clone expressing PDE5A shRNA. The data are presented relative to their respective empty vector control clones (dotted line). (E) Intracellular-free Ca^{2+} in 501mel cells treated with Sp-8-Br-PET-cGMPS (Br-cGMP; 100 μM), 8-pCPT-cGMP (8-pCPT; 50 μM), sodium nitroprusside (SNP; 100 μM), YC-1 (0.2 μM), tadalafil (Tad; 0.1 μM), sildenafil (Sil; 1 μM), or vardenafil (Var; 5 μM). The data are presented relative to vehicle-treated controls (H_2O for SNP; DMSO for all other compounds; dotted line). (F) Invasion of A375M2 cells was measured following treatment with DMSO (D), or the indicated concentrations of BAPTA (μM). (G) Invasion of 501mel cells was measured following transfection with scrambled control (SC) or PDE5A siRNA and treated with DMSO (D) or BAPTA (0.1 μM). (H) Invasion of 501mel cells was measured following transfection with scrambled control (SC) or PDE5A siRNA and treated with DMSO (D) or A23187 (0.5 μM). Invasion is presented relative to the scrambled control transfected, DMSO-treated cells. (I) Invasion was measured in A375M2 and WM266.4 cells treated with DMSO (D) or A23187 (0.2 μM). Error bars indicate ± standard error. ***$p < 0.001$, **$p < 0.01$, *$p < 0.05$. See also Figure S3.

PDE5A Regulates Melanoma Cell Invasion through cGMP, Ca^{2+}, and Increased Contractility

Next, we examined how PDE5A regulates invasion. We confirmed that stable re-expression of PDE5A caused the expected reduction in cytosolic cGMP in A375 and WM266.4 cells, whereas stable depletion of PDE5A by shRNA increased cGMP in 501mel cells (Figure 5A). Transient PDE5A depletion by siRNA also caused a substantial increase in cGMP in 501mel cells, as did the PDE5A inhibitors sildenafil, tadalafil, and vardenafil (Figure 5B). The difference in magnitude of response of 501mel cells to shRNA and siRNA presumably reflects differences in knockdown efficiency and cell adaptations to long-term protein loss. Importantly, two cell permeable cGMP analogs (Sp-8-Br-PET-cGMPS, 8-pCPT-cGMP) and two activators of soluble guanylate cyclases (YC-1, sodium nitroprusside [SNP]) induced 501mel cell invasion (Figure 5C), establishing that cGMP induces invasion in these cells. This was unexpected because melanoma cell invasion requires the forces generated by actin-myosin contractility (Pinner and Sahai, 2008; Sahai and Marshall, 2003), and in VSM cells, cGMP suppresses contractility (Surks, 2007). Therefore, we investigated how cGMP regulates melanoma cell invasion.

First, we examined PRKG1 and PRKG2 because PRKG1 induces cytoskeletal relaxation through Ca^{2+} in VSM cells. However, although PRKG1 was expressed in NHM, it was not expressed in melanoma cells (Figures S3A and S3B), and in agreement with this, PRGK1 siRNA did not affect invasion in 501mel cells (data not shown). We also found PRKG2 to be undetectable in both melanocytes and melanoma cells (data not shown). We next examined the cGMP-regulated, cAMP-specific phosphodiesterases PDE2, PDE3A, and PDE3B. Their expression varied greatly in melanoma cells (Figures S3C–S3E), and siRNA against them did not produce consistent effect on invasion (data not shown). We conclude that the cGMP effectors PRGK1/2, PDE2, PDE3A, and PDE3B do not regulate

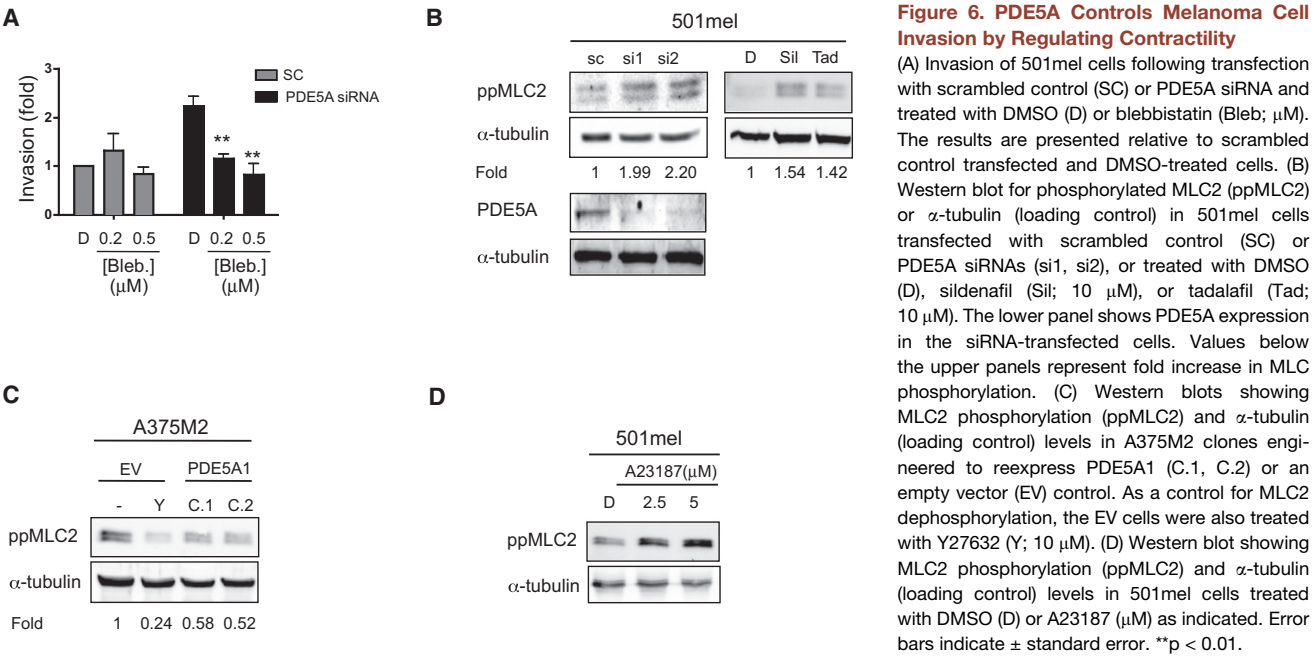

Figure 6. PDE5A Controls Melanoma Cell Invasion by Regulating Contractility

(A) Invasion of 501mel cells following transfection with scrambled control (SC) or PDE5A siRNA and treated with DMSO (D) or blebbistatin (Bleb; μM). The results are presented relative to scrambled control transfected and DMSO-treated cells. (B) Western blot for phosphorylated MLC2 (ppMLC2) or α-tubulin (loading control) in 501mel cells transfected with scrambled control (SC) or PDE5A siRNAs (si1, si2), or treated with DMSO (D), sildenafil (Sil; 10 μM), or tadalafil (Tad; 10 μM). The lower panel shows PDE5A expression in the siRNA-transfected cells. Values below the upper panels represent fold increase in MLC phosphorylation. (C) Western blots showing MLC2 phosphorylation (ppMLC2) and α-tubulin (loading control) levels in A375M2 clones engineered to reexpress PDE5A1 (C.1, C.2) or an empty vector (EV) control. As a control for MLC2 dephosphorylation, the EV cells were also treated with Y27632 (Y; 10 μM). (D) Western blot showing MLC2 phosphorylation (ppMLC2) and α-tubulin (loading control) levels in 501mel cells treated with DMSO (D) or A23187 (μM) as indicated. Error bars indicate ± standard error. **$p < 0.01$.

invasion in melanoma cells. In contrast, Ca^{2+} does appear to be important. Re-expression of PDE5A1 in A375 cells reduced intracellular Ca^{2+}, whereas its depletion in 501mel cells increased intracellular Ca^{2+} (Figure 5D). We show that Sp-8-Br-PET-cGMPS, 8-pCPT-cGMP, YC-1, and SNP all increased intracellular Ca^{2+} in 501mel cells (Figure 5E), and importantly, sequestration of intracellular Ca^{2+} by the cell-permeable chelator BAPTA suppressed A375 cell invasion (Figure 5F) and 501mel cell invasion induced by PDE5A depletion (Figure 5G). Conversely, 501mel cell invasion was substantially increased when intracellular Ca^{2+} was elevated using the calcium ionophore A23187 in 501mel cells (Figures 5H and S3F). However, note that A23187 did not further increase 501mel cell invasion following PDE5A depletion (Figure 5H) and did not increase invasion of A375M2 or WM266.4 cells (Figure 5I), which do not express PDE5A (Figures 1C and 1D).

Ca^{2+} has previously been implicated in invasion because it stimulates myosin light chain 2 (MLC2) phosphorylation, thereby inducing contractility (Somlyo and Somlyo, 2003). Therefore, we examined if Ca^{2+} regulated contractility in melanoma cells. First, we established that actin-myosin contractility was essential for invasion induced by PDE5A depletion in 501mel cells by showing that it was blocked by blebbistatin, a small molecule inhibitor of non-muscle myosin IIA (Figure 6A). We also show that PDE5A depletion by siRNA, or its inhibition by sildenafil and tadalafil, increased MLC2 phosphorylation in 501mel cells (Figure 6B). Conversely, MLC2 phosphorylation decreased when PDE5A was reexpressed in A375 cells (Figure 6C). A375 invasion and contractility have also been shown to be regulated by the Rho-kinases ROCKI and ROCKII (Sahai and Marshall, 2003), and notably, the reduction in MLC2 phosphorylation observed following PDE5A re-expression was similar to that seen when A375 cells were treated with the ROCK inhibitor Y27632 (Figure 6C). Finally, we also show that A23187 induces MLC2 phosphorylation in 501mel cells (Figure 6D).

PDE5A Regulates Melanoma Cell Invasion In Vivo

We next used intravital imaging to investigate the role of PDE5A in regulating melanoma cell invasion in vivo. WM266.4 cells expressing green fluorescent protein (WM266.4-GFP) were engineered to reexpress PDE5A1 (WM266.4-GFP/PDE5A1) and injected subcutaneously into the flanks of nude mice to establish palpable xenografts (3–4 weeks). The mice were anesthetized, and the movement of the fluorescently tagged cells in the tumors was recorded using two-photon microscopy. Images from representative videos of tumors of WM266.4-GFP and WM266.4-GFP/PDE5A cells are shown (Figure 7A), and to demonstrate cell motion the cells in still images taken from these videos at 0, 11, and 22 min were false colored red, green, or blue (RGB) and superimposed (Figure 7B). In these compilation images the red, green, and blue images of non-migrating cells overlap, making them appear white. In contrast the red, green, and blue images of migrating cells do not overlap, making them appear colored. The results of this analysis show that WM266.4-GFP cells were migrating, whereas WM266.4-GFP/PDE5A cells were not (Figure 7B). To quantify the migration, the number of individual moving cells in 40 (WM266.4-GFP) or 34 (WM266.4-GFP/PDE5A) movies from 8 tumors for each cell type was counted. The results (number of cells moving/mm^2/hr) corroborate the RGB analysis and show that PDE5A1 re-expression strongly suppressed the in vivo migratory behavior of WM266.4 cells ($p \leq 0.0033$; Figure 7C). Importantly, we confirm that PDE5A1 expression is not lost during the course of these in vivo experiments (Figure 7D).

In addition to being important for metastatic spread, cancer cells also need to invade to colonize distant sites. To examine this aspect of metastatic spread, we used a short-term lung colonization assay to investigate the in vivo consequences of PDE5A expression. For these studies we used WM266.4-GFP/PDE5A cells and as a control WM266.4 cells expressing cherry-red fluorescent protein (WM266.4-chRFP). These cells

were mixed in equal proportions and injected into the tail veins of nude mice. At various times the lungs from the mice were examined for the presence of the GFP and chRFP-expressing cells. Thirty minutes after injection, there were similar numbers of WM266.4-chRFP than WM266.4-GFP/PDE5A-expressing cells in the lung parenchyma of the recipient mice, but within 6 hr a greater proportion of WM266.4-chRFP cells remained (Figures 7E and 7F). Using analogously engineered A375 cells (A375-chRFP, A375-GFP/PDE5A), we show that PDE5A expression also reduces persistence of these cells in the lungs (Figure 7G).

We next examined the long-term consequences of PDE5A expression. We recently described a mouse model of melanoma driven by ^{V600E}Braf expressed from the endogenous mouse gene (Dhomen et al., 2009). We show that endogenous Pde5a1 is upregulated by PD184352 and U0126 in cells derived from these tumors (Figure 7H), demonstrating that the mouse *Pde5a* gene is also downregulated by oncogenic Braf in melanoma cells. We engineered these cells to express human PDE5A1 (4599.PDE5A cells; Figure 7I) and injected the cells into the tail veins of nude mice. Strikingly, PDE5A1 expression caused a substantial reduction in lung colonization by these cells, as demonstrated by the reduced weight of the lungs from the mice that received the PDE5A1-expressing cells, compared to the nonexpressing cells (Figure 7J). Thus, Pde5a/PDE5A downregulation increases lung colonization by melanoma cells, so we tested if PDE5A inhibition would achieve similar results. 4599.PDE5A cells were injected into the tail veins of mice that received sildenafil 1 hr prior to cell injection and then daily for the following 7 days. The lungs were harvested after a further 7 days, and the results show that sildenafil did not increase tumor burden (Figure 7K).

PDE5A Is Downregulated in Metastatic Melanoma

Finally, we used immunohistochemistry (IHC) to examine PDE5A expression in a tissue microarray (TMA) containing triplicate samples for 28 primary and 29 metastatic melanomas. Each sample was scored blind for intensity as low (score of one), intermediate (score of two), or high (score of three) (Figure 8A). We found a statistically significant ($p \leq 0.037$) correlation with PDE5A expression and tumor grade, with the primary tumors showing higher overall PDE5A expression than the metastatic tumors (Figure 8B).

DISCUSSION

The ability of cancer cells to migrate within a tumor and invade the surrounding matrix is thought to be critical to the process of metastatic spread. Previous studies have implicated oncogenic BRAF in melanoma metastasis but without elucidating the underlying mechanism(s) (Hingorani et al., 2003; Liang et al., 2007). We now show that one of the key steps in BRAF-induced invasion in melanoma cells appears to be downregulation of the cGMP phosphodiesterase PDE5A. Our interest in PDE5A was kindled when we identified it as potentially being downregulated by oncogenic BRAF in melanoma cells (Packer et al., 2009), suggesting a negative role in melanoma progression. Here, we confirm that oncogenic BRAF downregulates PDE5A in melanoma cells.

We previously demonstrated that ^{V600E}BRAF increases expression of the transcription factor BRN2 in melanoma cells (Goodall et al., 2004). BRN2 upregulation is associated with increased melanoma cell invasion (Pinner et al., 2009), and it was also recently shown to suppresses the expression of several genes (Kobi et al., 2010). We now show that BRN2 binds to the PDE5A promoter and using reporter constructs show that one of the putative BRN2-binding sites in the promoter is essential for the suppression of *PDE5A* transcription by oncogenic BRAF. We show that BRN2 depletion increases *PDE5A* transcription in melanoma cells, whereas PDE5A re-expression downregulates PDE5A in melanocytes. Thus, we establish a direct link between oncogenic BRAF, BRN2, and the regulation of *PDE5A* transcription, and we add *PDE5A* to the list of genes that are downregulated by BRN2. We note that BRN2 is upregulated in small cell lung cancer and neuroblastoma (Schreiber et al., 1992, 1994), raising the possibility that BRN2 could also regulate PDE5A expression and invasions in those cancers. Furthermore, because BRN2 is expressed in melanoblasts (Cook et al., 2003; Yamaguchi et al., 2007), the highly migratory melanocyte precursors, our data suggest that BRN2 may also regulate melanoblast migration through PDE5A during development.

Previously, studies have shown that Ca^{2+} regulates migration and metastasis of breast cancer cells (Yang et al., 2009), and we now establish that PDE5A regulates invasion of melanoma cells by regulating intracellular Ca^{2+} through cGMP. We show that cGMP and Ca^{2+} levels are inversely correlated with PDE5A expression in melanoma cells and that cGMP elevates Ca^{2+} in 501mel cells. The changes in cGMP and Ca^{2+} that we describe may appear modest, but we measured total cytosolic levels of these second messengers, and as has been established in cAMP signaling (Houslay, 2010), the actual changes in cGMP are likely to be restricted to local microdomains where the effective changes in concentration will be considerably higher. We were unable to determine the subcellular localization of PDE5A in the cells to establish the existence of these microdomains (data not shown), but importantly, we did show that artificially increasing either cGMP or Ca^{2+} using a variety of pharmacological agents was sufficient to induce 501mel cell invasion. Conversely, Ca^{2+} sequestration was sufficient to inhibit A375 cell invasion and invasion induced in 501mel cells when PDE5A was depleted. Our initial attempts to identify the cGMP-gated calcium channels responsible for regulating Ca^{2+} in melanoma cells were unsuccessful (possibly due to redundancy), but nevertheless, our data reveal a direct link between cGMP metabolism by PDE5A, intracelllular Ca^{2+}, and invasion downstream of oncogenic BRAF in melanoma cells. Notably, this response appears to be specific to BRAF mutant melanoma cells. It was not seen in NRAS mutant melanoma cells, or BRAF mutant colorectal cells. A reason for the difference with colorectal cells could be that they do not express BRN2, but it is still curious that MEK inhibition increased rather than reduced invasion in these cells. Clearly, more studies are needed to understand invasion in NRAS mutant melanoma and BRAF mutant colorectal cells.

Melanoma cells escape the tumor and invade the surrounding tissue using forces generated by actin-myosin contractility (Pinner and Sahai, 2008; Sahai and Marshall, 2003), and indeed, increased contractility drives melanoma invasion (Carreira et al.,

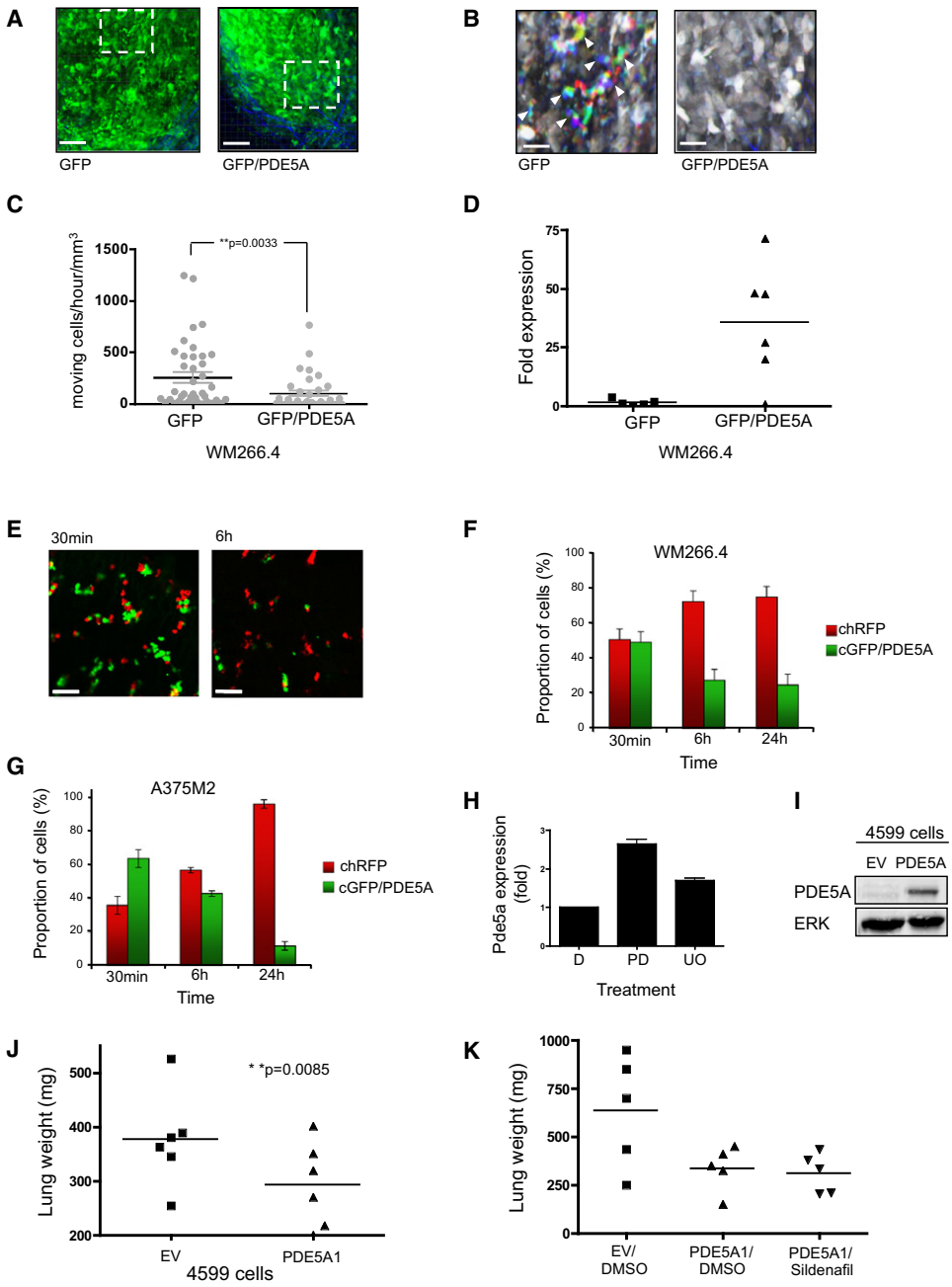

Figure 7. PDE5A Regulates Melanoma Cell Invasion In Vivo

(A) Low-resolution still images taken from video recordings of subcutaneous tumors formed from WM266.4-GFP (GFP) or WM266.4-GFP/PDE5A (GFP/PDE5A) cells. Scale bar, 80 μm. (B) High-resolution images of the region highlighted in the dotted boxes in (A). Three images of the cells were taken at 0, 11, and 22 min, false colored red, green, and blue, respectively, and then overlaid. Scale bar, 30 μm. (C) Quantification of moving cells (cells/hr/mm^2) of 40 movies from 8 tumors formed using WM266.4-GFP (GFP) or WM266.4-GFP/PDE5A (GFP/PDE5A) cells. The solid bars represent the average number of moving cells for the two populations with error bars to represent standard deviations from the mean. (D) PDE5A1 mRNA expression in WM266.4-GFP (GFP) or WM266.4-GFP/PDE5A (GFP/PDE5A) tumors was determined by qRT-PCR. Five tumors for each cell type were analyzed in triplicate, and average values for individual tumors are shown, relative to the value for endogenous PDE5A in WM266.4-GFP cells. The bars represent the average level for each tumor group. (E) Fluorescent images of WM266.4-chRFP (red) or WM266.4-GFP/PDE5A (green) cells in the lungs of mice 30 min or 6 hr after injection with equal number of each line. Scale bar, 75 μm. (F) Quantification of 10 fields of cells/lung from 3 mice 30 min, 6 hr, or 24 hr after injection with equal numbers of WM266.4-chRFP (chRFP) or WM266.4-GFP/PDE5A (GFP/PDE5A) cells. (G) Quantification of 10 fields of cells/lung from 3 mice 30 min, 6 hr, or 24 hr after injection with equal numbers of A375M2-chRFP (chRFP) or A375M2-GFP/PDE5A (GFP/PDE5A) cells. (H) Expression of Pde5a mRNA quantified by qRT-PCR in ^{V600E}Braf-expressing 4599-mouse melanoma cells treated with DMSO (D), PD184352 (PD; 1 μM), or U0126 (U0; 10 μM) for 24 hr. (I) Western blot showing PDE5A1 and ERK2 (loading control) levels in 4599 melanoma cells engineered for stable expression of PDE5A1 or an empty vector (EV) control. (J) Lung weights from mice following tail vein injection of 4599 melanoma cells expressing empty vector (EV) or PDE5A1. The weights of the individual lungs are shown, with the bars representing the mean

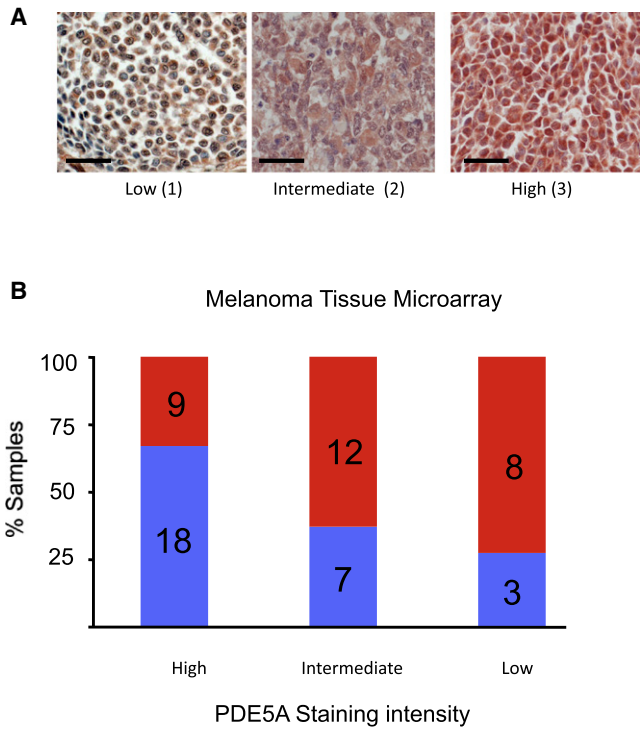

Figure 8. PDE5A Is Downregulated in Metastatic Melanoma

(A) Representative photomicrograph of the three grades of staining intensity used to score PDE5A expression in tissue microarrays. Scale bar, 25 μm. (B) Proportion (%) of tumor samples stained for high, intermediate, and low PDE5A in a tissue microarray consisting of triplicate cores of 28 primary (blue segments of bars) and 29 metastatic malignant (red segments of bars) melanoma cases. The numbers within the bars represent the number of samples found in each group.

2006). We show that PDE5A downregulation in 501mel cells increases contractility (shown by increased MLC2 phosphorylation) and induces invasion, whereas PDE5A re-expression in A375 cells reduces contractility (MLC2 dephosphorylation) and impairs invasion. Although the changes observed in MLC2 phosphorylation also appear modest, they are similar to the levels previously reported by others (Gadea et al., 2008; Krndija et al., 2010), and we confirm that contractility is essential for invasion in PDE5A-depleted melanoma cells because it is inhibited by blebbistatin. The induction of contractility following PDE5A depletion or inhibition in melanoma cells was unexpected because in VSM cells the opposite appears to occur. Specifically, cGMP induces relaxation rather than contractility in VSM cells (Surks, 2007), and it was recently shown that PDE5A inhibition by Pak causes RhoA downregulation, also leading to relaxation (Sauzeau et al., 2010). A notable difference between VSM and melanoma cells is that whereas PRKG1 modulates cGMP responses in VSM cells, PRKG1 (and PRKG2) is not expressed in melanoma cells.

PDE5A stimulates leukemia, colorectal carcinoma, and breast cancer cell proliferation and survival (Sarfati et al., 2003; Tinsley et al., 2009; Zhu et al., 2005), identifying it as a potential therapeutic target in cancer. We also found that PDE5A downregulation slowed the growth of some melanoma cells, but the major impact of its downregulation or inhibition was to induce invasion. Proliferation and invasion are inversely related in breast cancer cells (Giampieri et al., 2009), and our data suggest that PDE5A balances these behaviors in melanoma cells. More pertinently, because PDE5A is generally downregulated in BRAF mutant melanoma cells, its inhibition would presumably be without impact. Thus, we conclude that PDE5A is not a therapeutic target in melanoma, and our data even raise the possibility that PDE5A drugs could promote melanoma metastasis. This is important because patients with small primary tumors or stage I/II disease often already have distant secondary metastases, and melanoma cells can rapidly evolve to become invasive (Balch and Cascinelli, 2001), so any acceleration to this process is undesirable.

However, we do not perceive this to be a problem. There are no reports linking these drugs to increased risk of melanoma metastasis, and we found that sildenafil did not increase mouse lung colonization by melanoma cells. Furthermore, PDE5A drugs are generally used as needed rather than persistently and are generally cleared rapidly ($T_{1/2}$ ~2 hr) because their effects must be short lived. Moreover, in addition to being able to degrade cGMP, phosphodiesterases appear to possess enzyme-independent functions, as implied by their interaction with many other cellular proteins (Houslay, 2010). Thus, we posit that complete loss of PDE5A protein is not akin to its transient and reversible inhibition that is mediated by drugs. Furthermore, as mentioned, because PDE5A is already downregulated in most BRAF mutant melanoma cases, its further inhibition is presumably not possible. Therefore, our data should be interpreted with care, and we do not immediately suggest that PDE5A inhibitors will drive melanoma metastasis. However, we caution that with the ever-widening clinical use of these drugs, it is not possible to discount this risk completely. Perhaps more compelling, recent data show that BRAF drugs can achieve dramatic clinical responses in patients with melanomas expressing mutant forms of BRAF (Flaherty et al., 2010). Our data suggest that in addition to being anti-proliferative, these drugs could be anti-invasive because BRAF inhibition would allow PDE5A re-expression.

In conclusion we provide improved insight into the biology of ^{V600E}BRAF signaling in melanoma cells, showing that this oncogene downregulates PDE5A through the transcription factor BRN2, leading to increased cGMP and Ca^{2+} and the induction of invasion through increased cell contractility. Clearly, PDE5A does not appear to be a therapeutic target in BRAF mutant melanoma.

EXPERIMENTAL PROCEDURES

Refer to Supplemental Experimental Procedures for detailed protocols.

Cell Culture and Transfection Procedures

NHMs were from Cascade Biologics Inc. (Portland, OR) and cultured as recommended. WM266.4, A375P, A375M2, Skeml28, Skmel24, Colo829,

weight for each population. (K) Lung weights from mice 14 days after tail vein injection of 4599 melanoma cells expressing empty vector (EV) or PDE5A1. The mice were treated with sildenafil (1.3 mg/kg) or (DMSO). Treatment was given 1 hr before the cells were injected and then daily for the following 7 days. The weights of individual lungs are shown, with bars to represent the mean weight for each population. Error bars indicate ± standard error. *$p < 0.05$.

Skeml5, Skmel13, MEL-HO, 501mel, and 4599 were cultured in DMEM (GIBCO/Invitrogen) supplemented with 10% fetal bovine serum (FBS).

For culture on thick collagen layers, 2.5 ml serum-free fibrillar bovine dermal collagen (2.3 mg/ml) was dispensed into 6 well tissue culture plates coated with bovine serum albumin. The collagen was coagulated at 37°C/10% CO_2 (30 min), then cells were seeded in DMEM/10% serum for 24 hr, washed into DMEM/0.1% serum for 16 hr prior, and treated.

For stable expression of GFP or RFP, cells were transfected with pEGFP-C1 or pchERFP (Clontech) for G418 selection (Sigma). For stable PDE5A1 expression, cells were transfected with pEF-PDE5A1 and pBabepuro for puromycin selection. PDE5A shRNA stable clones (SA Biosciences) were selected by hygromycin and BRN2 expression and luciferase assays have been described (Wellbrock et al., 2008). For transient depletion of specific proteins, cells were transfected with 20 nM siRNA oligonucleotides (sequences in Supplemental Experimental Procedures) using LipofectAMINE (GIBCO/Invitrogen).

In Vitro Invasion Assays

A total of 5 × 10^3 cells in 100 μl serum-free collagen I at 2.3 mg/ml was dispensed into 96-well ViewPlates (Perkin-Elmer, UK) coated with bovine serum albumin. The cells were sedimented at 300 × g and incubated at 37°C/10% CO_2 for 30 min to coagulate the collagen, then overlaid with DMEM/10% FBS. After 24 hr, cells were fixed (4% formaldehyde) and stained with Hoechst 33258 (Invitrogen). Confocal Z sections were collected at the bottom of the wells and at 50 μm in an INCELL3000 high-content microscope. Nuclear staining was quantified with INCELL3000 software with the Object Intensity module. Invasion indices = [cells at 50 μm]/[cells at 1 μm]. Means of quadruplicate samples are presented as fold compared to controls.

Biochemical Techniques

Western blots were performed by standard techniques using fluorescent-labeled secondary antibodies (Invitrogen; or Li-COR Biosciences) and analyzed on an Odyssey Infrared Scanner (Li-COR Biosciences). The antibodies used were: rabbit anti-PDE5A (H-120, sc-32884), rabbit anti-ERK2 (C-14, sc-154), mouse anti-BRAF (F-7, sc-5284), and goat anti-(BRN2 (C-20, SC-6029) from Santa Cruz; mouse anti-α-tubulin and mouse anti-phospho-ERK2 (M8159) from Sigma; mouse anti-MEK2 (clone 96, 610235) from BD Biosciences; rabbit anti-phosphoMLC2 (ser19) (3671) from Cell Signaling (Cambridge-Biosciences); and rabbit anti-PKGI (KAP-PK005D) from Stressgen (Cambridge-Biosciences). PD184352 and PLX4720 were synthesized in-house, SB590885 was from Symansis (Auckland, New Zealand), and UO126 from Promega. A23187 and BAPTA were from Tocris. Ca^{2+} concentration was measured using Fluo-4mDirect Calcium Assay kits (Invitrogen) and cGMP using Direct cGMP kits (Biomol).

Quantitative Real-Time PCR

RNA extracted from 2 × 10^5 cells by RNeasy Kits (QIAGEN) was reverse transcribed to generate cDNA using M-MLV Reverse Transcriptase (Sigma). Quantitative real-time PCR was performed using Precision Mastermix (PrimerDesign) and TaqMan Gene Expression Assay probes on an Applied Biosystems 7900HT Fast Real Time Machine (Applied Biosystems). Relative expression was calculated using the ΔΔCt method and β-2 microglobulin as an internal control.

In Vivo Studies

All procedures involving animals were approved by the Animal Ethics Committees of the Institute of Cancer Research and the CR-UK London Research Institute in accordance with National Home Office regulations under the Animals (Scientific Procedures) Act 1986 and according to the guidelines of the Committee of the National Cancer Research Institute (Workman et al., 2010). For xenografts, 1 × 10^6 cells in 0.1 ml PBS were inoculated subcutaneously into the flanks of female (five per group) CD1 nude mice (Charles River; UK). Tumor volumes were determined using volume = length × width × depth (mm) × 0.5236. For short-term lung colonization assays, 5 × 10^5 cells expressing GFP or chRFP (each) were mixed in 100 μl PBS and injected into the tail veins of nude mice. Mice were sacrificed after 30 min, 6 hr, or 24 hr, and the surface of the lungs was examined for GFP or chRFP-expressing cells. Cell numbers (average of ten measurements per lung, three mice per experiment) are expressed as percentage of total number of cells counted. For long-term lung colonization, 1 × 10^6 4599.EV or 4599.PDE5A1 cells in 100 μl PBS were injected into the tail veins of nude mice, and the lungs were weighed after 14 days.

For intravital imaging, 1 × 10^6 WM266.4-GFP/PDE5A1 or WM266.4-GFP cells were injected subcutaneously into the flank of nude mice. When tumors were 3–7 mm^2, the mice were anesthetized, and the tumors were exposed to a two-photon microscope for video imaging. To quantify movement, several regions from eight tumors were video recorded for 25 min, and moving cells were defined as those that moved 10 μm or more during the video period.

IHC

All procedures using human tissues were approved by the Ethics Committees of the Institute of Cancer Research and the Royal Marsden Hospital Foundation Trust in accordance with the Human Tissue Act 2004 (c.30). The high-density melanoma tissue microarray (Tissue Microarray ME207 061) was purchased from Biomaxx (Rockville, MD, USA) and contains multiple primary and metastatic melanoma samples collected with full donor consent under IRB and HIPPA-approved protocols.

PDE5A antigen was retrieved by microwave (18 min in citrate buffer) and detected with rabbit polyclonal antibody (PDE5A; NBP1-00639, Novus Biologicals Inc., 1:50) and the Vectastain Elite ABC kit (Vector Laboratories). The samples were blind scored by A.V. as low (1), intermediate (2), or high (3), and scores were validated in 30 randomly selected cores by B.S.-L. Interobserver agreement was excellent (kappa score >0.8). Average staining intensity per sample is presented.

Statistical Analysis

The Student's t test was performed for mRNA expression, fold-invasive index, cell adhesion, and lung extravasation assays, the Mann Whitney *U* test was performed for the scatter plots, and the chi-square test was performed for the TMAs.

SUPPLEMENTAL INFORMATION

Supplemental Information includes Supplemental Experimental Procedures and three figures and can be found with this article online at doi:10.1016/j.ccr.2010.10.029.

ACKNOWLEDGMENTS

This work was supported by Cancer Research UK (ref: C107/A10433), The Institute of Cancer Research, The Harry J Lloyd Charitable Trust, and a FEBS (Federation of European Biochemical Societies) Long Term Fellowship (B.S.-L.).

Received: April 21, 2010
Revised: August 30, 2010
Accepted: October 14, 2010
Published online: January 6, 2011

REFERENCES

Balch, C.M., and Cascinelli, N. (2001). The new melanoma staging system. Tumori *87*, S64–S68.

Biel, M., and Michalakis, S. (2009). Cyclic nucleotide-gated channels. Handb. Exp. Pharmacol. *191*, 111–136.

Carreira, S., Goodall, J., Denat, L., Rodriguez, M., Nuciforo, P., Hoek, K.S., Testori, A., Larue, L., and Goding, C.R. (2006). Mitf regulation of Dia1 controls melanoma proliferation and invasiveness. Genes Dev. *20*, 3426–3439.

Cook, A.L., Donatien, P.D., Smith, A.G., Murphy, M., Jones, M.K., Herlyn, M., Bennett, D.C., Leonard, J.H., and Sturm, R.A. (2003). Human melanoblasts in culture: expression of BRN2 and synergistic regulation by fibroblast growth factor-2, stem cell factor, and endothelin-3. J. Invest. Dermatol. *121*, 1150–1159.

Davies, H., Bignell, G.R., Cox, C., Stephens, P., Edkins, S., Clegg, S., Teague, J., Woffendin, H., Garnett, M.J., Bottomley, W., et al. (2002). Mutations of the BRAF gene in human cancer. Nature *417*, 949–954.

Dhomen, N., Reis-Filho, J.S., da Rocha Dias, S., Hayward, R., Savage, K., Delmas, V., Larue, L., Pritchard, C., and Marais, R. (2009). Oncogenic Braf induces melanocyte senescence and melanoma in mice. Cancer Cell *15*, 294–303.

Dumaz, N., and Marais, R. (2005). Integrating signals between cAMP and the RAS/RAF/MEK/ERK signalling pathways. Based on the anniversary prize of the Gesellschaft fur Biochemie und Molekularbiologie Lecture delivered on 5 July 2003 at the Special FEBS Meeting in Brussels. FEBS J. *272*, 3491–3504.

Flaherty, K.T., Puzanov, I., Kim, K.B., Ribas, A., McArthur, G.A., Sosman, J.A., O'Dwyer, P.J., Lee, R.J., Grippo, J.F., Nolop, K., et al. (2010). Inhibition of mutated, activated BRAF in metastatic melanoma. N. Engl. J. Med. *363*, 809–819.

Gadea, G., Sanz-Moreno, V., Self, A., Godi, A., and Marshall, C.J. (2008). DOCK10-mediated Cdc42 activation is necessary for amoeboid invasion of melanoma cells. Curr. Biol. *18*, 1456–1465.

Ghofrani, H.A., Osterloh, I.H., and Grimminger, F. (2006). Sildenafil: from angina to erectile dysfunction to pulmonary hypertension and beyond. Nat. Rev. Drug Discov. *5*, 689–702.

Giampieri, S., Manning, C., Hooper, S., Jones, L., Hill, C.S., and Sahai, E. (2009). Localized and reversible TGFbeta signalling switches breast cancer cells from cohesive to single cell motility. Nat. Cell Biol. *11*, 1287–1296.

Goodall, J., Wellbrock, C., Dexter, T.J., Roberts, K., Marais, R., and Goding, C.R. (2004). The Brn-2 transcription factor links activated BRAF to melanoma proliferation. Mol. Cell. Biol. *24*, 2923–2931.

Goodall, J., Carreira, S., Denat, L., Kobi, D., Davidson, I., Nuciforo, P., Sturm, R.A., Larue, L., and Goding, C.R. (2008). Brn-2 represses microphthalmia-associated transcription factor expression and marks a distinct subpopulation of microphthalmia-associated transcription factor-negative melanoma cells. Cancer Res. *68*, 7788–7794.

Gray-Schopfer, V., Wellbrock, C., and Marais, R. (2007). Melanoma biology and new targeted therapy. Nature *445*, 851–857.

Hingorani, S.R., Jacobetz, M.A., Robertson, G.P., Herlyn, M., and Tuveson, D.A. (2003). Suppression of BRAF(V599E) in human melanoma abrogates transformation. Cancer Res. *63*, 5198–5202.

Houslay, M.D. (2010). Underpinning compartmentalised cAMP signalling through targeted cAMP breakdown. Trends Biochem. Sci. *35*, 91–100.

Karasarides, M., Chiloeches, A., Hayward, R., Niculescu-Duvaz, D., Scanlon, I., Friedlos, F., Ogilvie, L., Hedley, D., Martin, J., Marshall, C.J., et al. (2004). B-RAF is a therapeutic target in melanoma. Oncogene *23*, 6292–6298.

Kasper, B., D'Hondt, V., Vereecken, P., and Awada, A. (2007). Novel treatment strategies for malignant melanoma: a new beginning? Crit. Rev. Oncol. Hematol. *62*, 16–22.

Kobi, D., Steunou, A.L., Dembélé, D., Legras, S., Larue, L., Nieto, L., and Davidson, I. (2010). Genome-wide analysis of POU3F2/BRN2 promoter occupancy in human melanoma cells reveals Kitl as a novel regulated target gene. Pigment Cell Melanoma Res. *23*, 404–418.

Krndija, D., Schmid, H., Eismann, J.L., Lother, U., Adler, G., Oswald, F., Seufferlein, T., and von Wichert, G. (2010). Substrate stiffness and the receptor-type tyrosine-protein phosphatase alpha regulate spreading of colon cancer cells through cytoskeletal contractility. Oncogene *29*, 2724–2738.

Liang, S., Sharma, A., Peng, H.H., Robertson, G., and Dong, C. (2007). Targeting mutant (V600E) B-Raf in melanoma interrupts immunoediting of leukocyte functions and melanoma extravasation. Cancer Res. *67*, 5814–5820.

Lin, C.S., Lin, G., Xin, Z.C., and Lue, T.F. (2006). Expression, distribution and regulation of phosphodiesterase 5. Curr. Pharm. Des. *12*, 3439–3457.

Lugnier, C. (2006). Cyclic nucleotide phosphodiesterase (PDE) superfamily: a new target for the development of specific therapeutic agents. Pharmacol. Ther. *109*, 366–398.

Mongillo, M., Tocchetti, C.G., Terrin, A., Lissandron, V., Cheung, Y.F., Dostmann, W.R., Pozzan, T., Kass, D.A., Paolocci, N., Houslay, M.D., et al. (2006). Compartmentalized phosphodiesterase-2 activity blunts beta-adrenergic cardiac inotropy via an NO/cGMP-dependent pathway. Circ. Res. *98*, 226–234.

Omori, K., and Kotera, J. (2007). Overview of PDEs and their regulation. Circ. Res. *100*, 309–327.

Packer, L.M., East, P., Reis-Filho, J.S., and Marais, R. (2009). Identification of direct transcriptional targets of (V600E)BRAF/MEK signalling in melanoma. Pigment Cell Melanoma Res. *22*, 785–798.

Pilz, R.B., and Broderick, K.E. (2005). Role of cyclic GMP in gene regulation. Front. Biosci. *10*, 1239–1268.

Pinner, S., and Sahai, E. (2008). PDK1 regulates cancer cell motility by antagonising inhibition of ROCK1 by RhoE. Nat. Cell Biol. *10*, 127–137.

Pinner, S., Jordan, P., Sharrock, K., Bazley, L., Collinson, L., Marais, R., Bonvin, E., Goding, C., and Sahai, E. (2009). Intravital imaging reveals transient changes in pigment production and Brn2 expression during metastatic melanoma dissemination. Cancer Res. *69*, 7969–7977.

Sahai, E., and Marshall, C.J. (2003). Differing modes of tumour cell invasion have distinct requirements for Rho/ROCK signalling and extracellular proteolysis. Nat. Cell Biol. *5*, 711–719.

Sanz-Moreno, V., Gadea, G., Ahn, J., Paterson, H., Marra, P., Pinner, S., Sahai, E., and Marshall, C.J. (2008). Rac activation and inactivation control plasticity of tumor cell movement. Cell *135*, 510–523.

Sarfati, M., Mateo, V., Baudet, S., Rubio, M., Fernandez, C., Davi, F., Binet, J.L., Delic, J., and Merle-Beral, H. (2003). Sildenafil and vardenafil, types 5 and 6 phosphodiesterase inhibitors, induce caspase-dependent apoptosis of B-chronic lymphocytic leukemia cells. Blood *101*, 265–269.

Sauzeau, V., Sevilla, M.A., Montero, M.J., and Bustelo, X.R. (2010). The Rho/Rac exchange factor Vav2 controls nitric oxide-dependent responses in mouse vascular smooth muscle cells. J. Clin. Invest. *120*, 315–330.

Schreiber, E., Himmelmann, A., Malipiero, U., Tobler, A., Stahel, R., and Fontana, A. (1992). Human small cell lung cancer expresses the octamer DNA-binding and nervous system-specific transcription factor N-Oct 3 (brain-2). Cancer Res. *52*, 6121–6124.

Schreiber, E., Merchant, R.E., Wiestler, O.D., and Fontana, A. (1994). Primary brain tumors differ in their expression of octamer deoxyribonucleic acid-binding transcription factors from long-term cultured glioma cell lines. Neurosurgery *34*, 129–135.

Somlyo, A.P., and Somlyo, A.V. (2003). Ca2+ sensitivity of smooth muscle and nonmuscle myosin II: modulated by G proteins, kinases, and myosin phosphatase. Physiol. Rev. *83*, 1325–1358.

Surks, H.K. (2007). cGMP-dependent protein kinase I and smooth muscle relaxation: a tale of two isoforms. Circ. Res. *101*, 1078–1080.

Tinsley, H.N., Gary, B.D., Keeton, A.B., Zhang, W., Abadi, A.H., Reynolds, R.C., and Piazza, G.A. (2009). Sulindac sulfide selectively inhibits growth and induces apoptosis of human breast tumor cells by phosphodiesterase 5 inhibition, elevation of cyclic GMP, and activation of protein kinase G. Mol. Cancer Ther. *8*, 3331–3340.

Wellbrock, C., Rana, S., Paterson, H., Pickersgill, H., Brummelkamp, T., and Marais, R. (2008). Oncogenic BRAF regulates melanoma proliferation through the lineage specific factor MITF. PLoS ONE *3*, e2734.

Workman, P., Aboagye, E.O., Balkwill, F., Balmain, A., Bruder, G., Chaplin, D.J., Double, J.A., Everitt, J., Farningham, D.A., Glennie, M.J., et al; Committee of the National Cancer Research Institute. (2010). Guidelines for the welfare and use of animals in cancer research. Br. J. Cancer *102*, 1555–1577.

Yamaguchi, Y., Brenner, M., and Hearing, V.J. (2007). The regulation of skin pigmentation. J. Biol. Chem. *282*, 27557–27561.

Yang, S., Zhang, J.J., and Huang, X.Y. (2009). Orai1 and STIM1 are critical for breast tumor cell migration and metastasis. Cancer Cell *15*, 124–134.

Zhu, B., Vemavarapu, L., Thompson, W.J., and Strada, S.J. (2005). Suppression of cyclic GMP-specific phosphodiesterase 5 promotes apoptosis and inhibits growth in HT29 cells. J. Cell. Biochem. *94*, 336–350.